



Project Summary

Impact of Topographic Circulations on the Transport and Dispersion of Air Pollutants

Richard T. McNider and Roger A. Pielke

A numerical mesoscale model was used to examine slope flows and classic mountain-plain air circulation for idealized topography. Special emphasis was given to turbulent parameterization in the stable boundary layer and to the unique characteristics of turbulent mixing in the slope flows. The numerical simulations for idealized valley-plain configurations produced results consistent with previously described observations, such as shallow sidewall flows, the pooling of cool air in the valley, and a deep mountain flow out of the valley. A Lagrangian particle model, operated in the terrain-following coordinate system of the mesoscale model, was developed to examine pollutant transport in the modeled circulations, while a Markov statistical process was used to evaluate turbulent dispersion. Higher order turbulence parameters needed for the statistical model were directly computed from the numerical model. Results of dispersion tests in the modeled slope flows showed enhanced vertical dispersion in the slope flows compared to flow over a flat boundary and, importantly, that normal surface scaling parameters for pollutant dispersion, such as friction velocity, were inappropriate for the slope flows.

This research was supported by U.S. Environmental Protection Agency Grant No. R806207010. Computer

support was provided by the National Center for Atmospheric Research, funded by the National Sciences Foundation.

This Project Summary was developed by EPA's Environmental Sciences Research Laboratory, Research Triangle Park, NC, to announce key findings of the research project that is fully documented in a separate report of the same title (see Project Report ordering information at back).

Introduction

The overall objective of this research was to use a mesoscale, primitive equation model [The University of Virginia Mesoscale Model (UVMM)] to produce dynamically consistent flow and turbulence fields in complex terrain. Model-predicted fields were then to be used to examine the transport and dispersion of pollutants. To accomplish the overall objective, some improvements to the mesoscale model were required to properly simulate drainage flows in complex terrain, and special techniques were developed to fully utilize the model flow and turbulence fields to examine point and area sources of pollution.

Modeling the Nocturnal Boundary Layer

In the past, use of the UVMM and most other mesoscale models has been

primarily directed towards examining the convective boundary layer of classic mountain-plain air circulation with an emphasis on sea breeze flows or heated up-slope flows. For polluted air, the stable boundary layer and drainage flows are generally the most restrictive to pollutant dispersal. Also, since drainage flows are themselves highly dependent upon vertical mixing processes, a good deal of effort was expended to incorporate an *accurate* nocturnal boundary layer formulation into the model. The formation chosen was a local exchange coefficient scheme proposed by Blackadar (1979). With some modification, this scheme has been included in the model.

This technique, in conjunction with a surface energy budget and a long-wave radiation parameterization, appeared to do as well in simulating the nocturnal boundary layer as the more complex numerical second-order closure schemes. A complete description of the local exchange coefficient model is given in McNider and Pielke (1981). McNider and Pielke also examine boundary-layer development over sloping terrain and show the importance of the terrain-induced pressure gradient and mixing processes to the generation of strong nocturnal jets.

The local mixing formulation allowed a dynamically consistent surface boundary layer and turbulent field to be generated over a terrain obstacle. The use of local conditions (based on local gradient Richardson number) was especially important to slope flow simulation, since the shear zones *above the surface* produce the mixing and entrainment into the drainage flow.

Slope Flows

In complex terrain, under synoptic conditions associated with large scale air stagnation, local mesoscale circulations provide the primary dilution and transport mechanisms for pollutants. To assess transport and dispersion of pollutants in complex terrain, the first step is to understand and model the mountain-valley wind systems. Defant (1951) provides an excellent summary of observations and descriptive models, including the characteristics of slope flows and the importance of these slope flows in producing an along-the-valley axis component (the true mountain wind).

The modeled valley has the classic mountain-plain configuration described by Defant, and was purposefully accen-

tuated to have a high height-to-width ratio (19 km wide, 2 km deep) with a sidewall slope of .25 (14°) (see Figure 1). Shallow drainage flows developed quickly over both sidewalls in response to surface cooling produced by a surface energy budget. The depth of the slope flow and height of the downslope velocity maximum (Figure 2) appeared to agree well with generic observations for similar slopes. However, the magnitude of the modeled velocity generally appeared larger than most observed maximums. In the model, an upslope return flow was also noted above the shallow downslope flow.

As mentioned, the slope flows developed rapidly, reaching their maximum within the first hour. These slope flows gradually produced a pooling of cool air in the valley. Later, downslope velocities decreased throughout the night in response to increased temperature stratification in the valley.

The turbulent exchange processes were directly linked to the developing flow fields. Downward moving air tended to deform the potential temperature field, producing a less stable profile

aloft. The return upslope flow accentuated this deformation, actually producing an unstable layer. Because the local turbulent exchange coefficients in the current model were dependent upon the local gradient Richardson number, this unstable layer, in conjunction with the wind shear near the top of the drainage flow, produced a highly turbulent zone aloft. Figure 3 shows the exchange coefficient profile and Richardson number over the slope.

Mountain Flows

According to Defant (1951), the mountain wind is driven by the slope flows, filling the valley with cooled air from the slopes. The pool of cool air creates a hydrostatic pressure gradient between the interior of the valley and plains outside the valley, causing a deep flow out of the valley. Because the slope flows are generally much shallower than the deep mountain wind, their importance to pollutant transport is probably secondary to the mountain wind that develops within a valley.

In the model (after starting with an adiabatic atmosphere) definite pooling

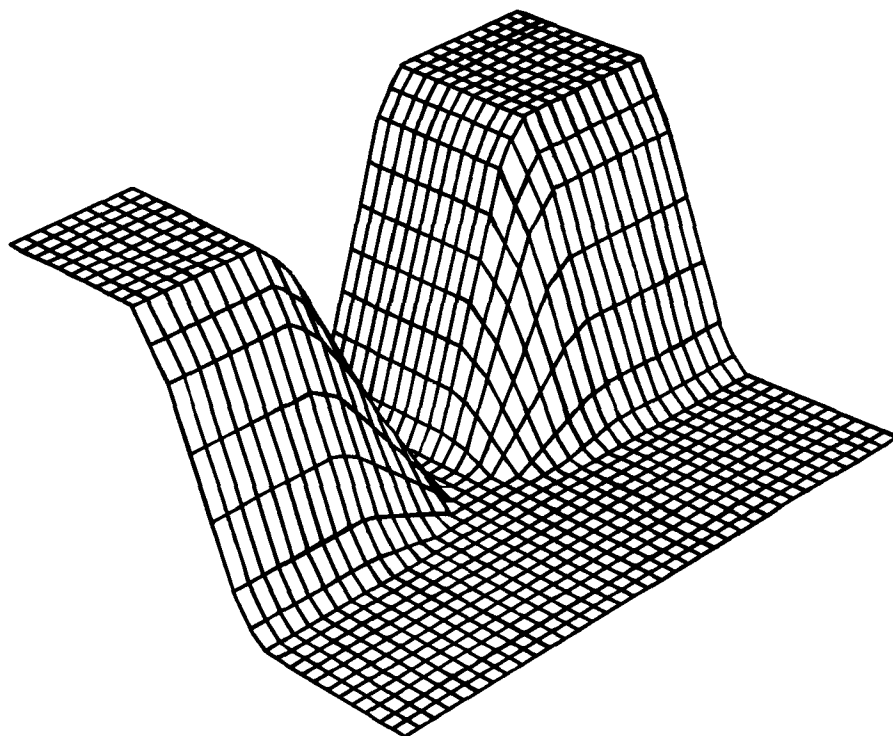


Figure 1. Three-dimensional perspectives of the topographic configuration used in Case A. Ridge height is 2 km; valley width is 19 km. (Note that the vertical scale is exaggerated.)

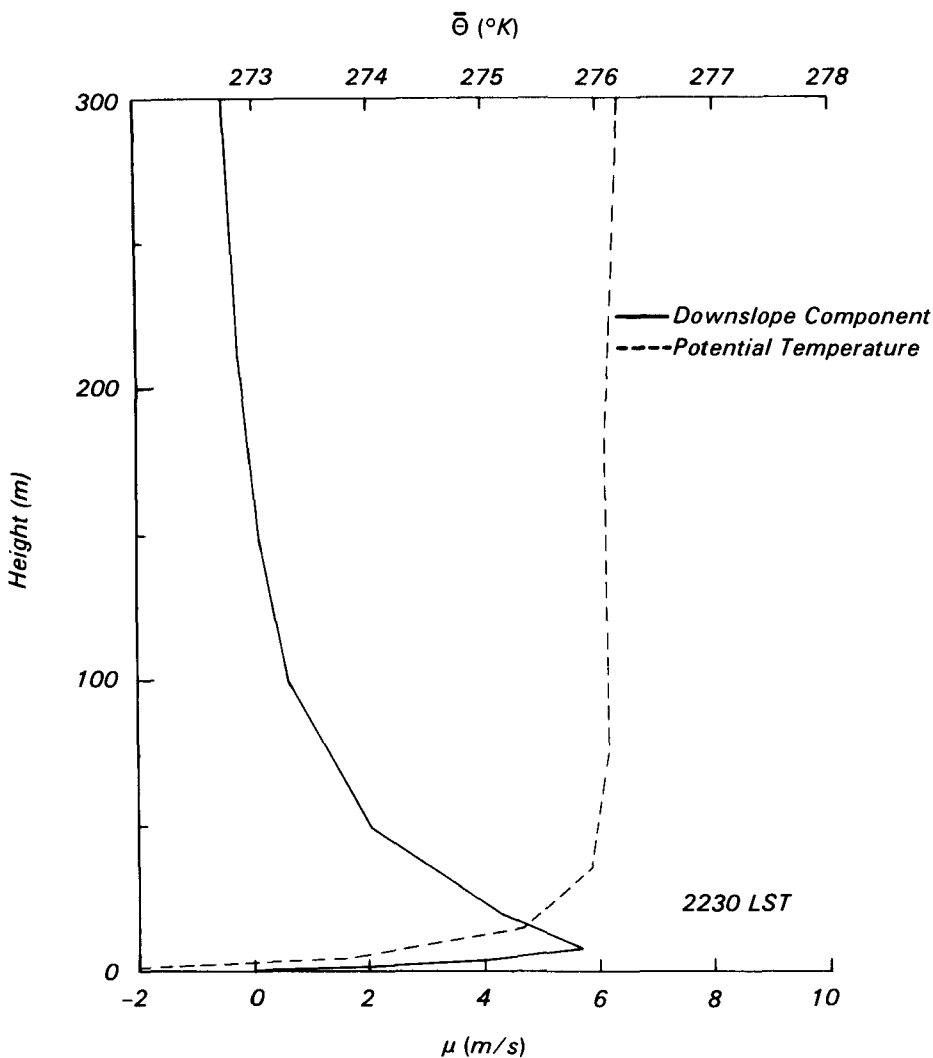


Figure 2. Downslope component and potential temperature profiles over the western sidewall of the two-dimensional valley at 0230 LST.

of the cooled air occurred, as illustrated in Figure 4a by the vertical gradient of potential temperature. The cooling in the valley was unusual because it did not appear to originate at the surface. Rather, cooling occurred at all heights within the valley, with the greatest cooling occurring near the surface. This appears to be consistent with the cooling pattern observed in deep valleys in Colorado (C. D. Whiteman, 1980). The pooling of cool air in the valley, consistent with Defant's descriptive model, produced a deep flow out of the valley. Figure 4b shows this deep mountain flow which extends to near ridge height.

Pollutant Transport

Most mesoscale flows, such as sea breeze and mountain-valley flows, are characterized by strong vertical shear (in both direction and speed) and horizontal variability. In order to examine pollutant transport in the mean mesoscale model wind field, a Lagrangian particle model was developed. The Lagrangian particle model used a volume-weighting scheme (Tuescher and Hauser, 1974) to interpolate model velocities in the variably spaced model grid to the particle position. Initial particle positions were transformed into the terrain-following coordinate system, and then advected in that system. For

display purposes, particles were back-transformed into a normal z system. The particle model could then produce streaklines as well as trajectories from various positions in the model flow. Figure 5 shows examples of streaklines produced by the particle model in a modeled sea breeze flow. A more complete description of the particle model and related experiments is given in McNider and Pielke (1979).

Grid Cell Pollutant Transport and Dispersion

Pollutant plumes with scales larger than both the model grid size and the dominant turbulent scales can be transported and diffused satisfactorily by using the advection equation and gradient transfer theory as follows:

$$\frac{\partial C}{\partial t} = -u_j \frac{\partial C}{\partial x_j} + \frac{\partial}{\partial x_i} \left(K \frac{\partial C}{\partial x_i} \right) \quad (1)$$

In the UVMM, a highly accurate advection scheme employing an upstream spline interpolation technique (Mahrer and Pielke, 1978) was used together with a forward time-weighted diffusion scheme (Paegle, et al., 1976) to solve Equation 1. Mean velocities and diffusion coefficients taken at mesoscale model grid points were used to transport and diffuse a passive pollutant. Figure 6 shows particle concentrations (emitted from an urban strip and area sources over the land) diffused and transported within a sea breeze flow using this scheme.

Point Source Transport and Diffusion

As previously mentioned, area sources can generally be included by using the conservation equation employing gradient transfer theory. However, point sources cannot be directly used in a coarse grid numerical model using Equation 1. This is due to numerical damping and the fact that plumes (small when compared to the turbulent scale) either do not diffuse in a gradient fashion, or require the effective exchange coefficient (K) to be a function of travel distance.

Due to the highly sheared environment and unsteady character of the local circulations, the subgrid scale plume dispersion could not be easily parameterized using analytical methods. An alternative used in the present investigation consisted of a conditioned particle dispersion scheme that Hanna

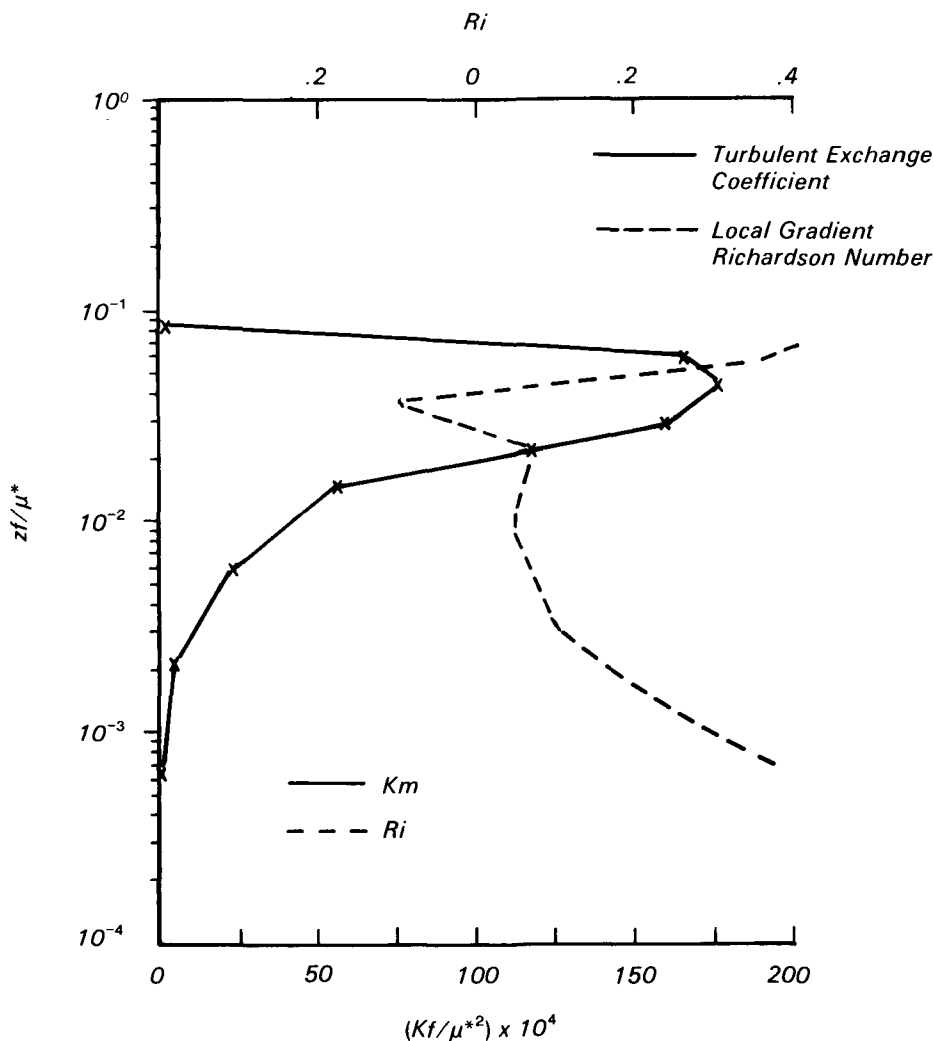


Figure 3. Turbulent exchange coefficient over the western valley wall showing pronounced maximum near the top of the slope flow and local gradient Richardson number showing the unstable layer aloft created by the deformation of the temperature field.

(1979) based upon Taylor's 1921 theorem for particle dispersion, in which the particle velocity (using the u-component as an example) is expressed by:

$$u_p = u + u' \quad (2)$$

where u = the mesoscale wind, and u' = a turbulent component given by:

$$u'(t + \tau) = u'(t) R(\tau) + u'' \quad (3)$$

The variable u'' is a random component dependent upon the turbulent energy, σ_u , and the autocorrelation function R . Use of this scheme required

an estimate of σ_u and R consistent with the model boundary layer. This was accomplished for the vertical component of the convective boundary layer using;

$$K_m = A \sigma_w \lambda_m \quad (4)$$

where λ_m = the spectral peak in the vertical velocity component, and

K_m = the model-predicted exchange coefficient for momentum.

In this convective boundary layer, the parameter λ_m was related to height and was limited to the model-predicted

boundary layer height. Figure 7 shows model-deduced σ_w values scaled appropriately for comparison with estimates from field observations in convective situations.

In the nocturnal boundary layer, σ_w was directly deduced from the second-order approximations of Blackadar (1979) as a function of local gradient Richardson number, and the length scale λ_m was made dependent upon the mixing length used in the exchange coefficient formulation. The autocorrelation function, R , needed in Equation 3, was taken to be exponentially dependent upon the Lagrangian time scale, which was in turn determined from λ_m and the mean wind speed. See McNider, et al. (1980) for complete details.

The conditioned particle diffusion scheme was well suited for the non-uniform wind and turbulence field generated by the mesoscale model, and allowed the turbulent dispersion to be consistent with the dynamic solution. Unlike some schemes, in which dispersion accuracy is lost in trying to use the conservation equation, the conditioned particle scheme is good or better than Gaussian models in uniform fields, but as mentioned earlier, can be applied to the sheared environment of drainage flows as well.

Transport and Dispersion in the Slope and Mountain Flows

Using the Lagrangian particle model, transport and dispersion of pollutants were examined in the slope and mountain flows produced by the mesoscale model. Particles were released at a height of 8 m on the western sidewall of the idealized valley depicted earlier. Figure 8 gives mean particle trajectories and shows the particles moving first towards the center of the valley, then out of the valley under the influence of the mountain wind.

Turbulent spread in the slope flows was also examined. To isolate the effect of the slope flows, a control experiment was conducted over a flat, slightly stable boundary layer. In the control experiment, particles were released within the boundary layer from a height of 8 m, then allowed to disperse without transport by a mean wind so shear-induced turbulence would not be a factor. Two similar experiments (one with a mean wind, one without) were undertaken within the slope flows previously described, with particles

released from a height of 8 m above the western sidewall. Figure 9 gives the root-mean-square vertical spread in the three experiments. Results indicated that dispersion rates were dramatically accelerated in the slope flows. The failure of the dispersion curves to coincide, which is to say dispersion is not a function of the friction velocity alone, points out that surface stress was not a good indication of turbulent energy in the slope flows.

Conclusions

The major result in this study was the success of a numerical model to reproduce the essential features of the classic mountain-plain circulation, including the deep mountain flow out of the valley. The success of the numerical experiment was readily expected since, unlike direct sea breeze circulations or slope flows, the mountain flow is a secondary circulation and a true three-dimensional feature. Part of the success in the simulations must be attributed to the turbulent parameterization scheme incorporated into the model, which avoided physically and numerically troublesome superadiabatic layers aloft as the cool air pools in the valley.

The second major result of this study was the finding that Lagrangian particle methods, coupled with the numerical mesoscale model could directly examine pollutant transport in the complex flow field, and could provide a robust method for explicitly incorporating parameters characterizing the turbulent dispersion. Techniques described in this investigation allowed these turbulent parameters to be computed directly from the mesoscale model so they were consistent with the dynamic solution.

The models and methodologies developed in this research should be useful for guiding the design or interpretation of dispersion experiments in complex terrain. Also, the models could be used to shorten or extend the parametric range of limited observations in complex terrain.

References

Blackadar, A.K., 1979. High Resolution Models of the Planetary Boundary Layer. In: *Advances in Environmental and Scientific Engineering*, Vol. 1, Gordon and Breach. pp. 50-81.

Deardorff, J., 1974. Three-Dimensional Numerical Study of the Height and Mean Structure of the Planetary

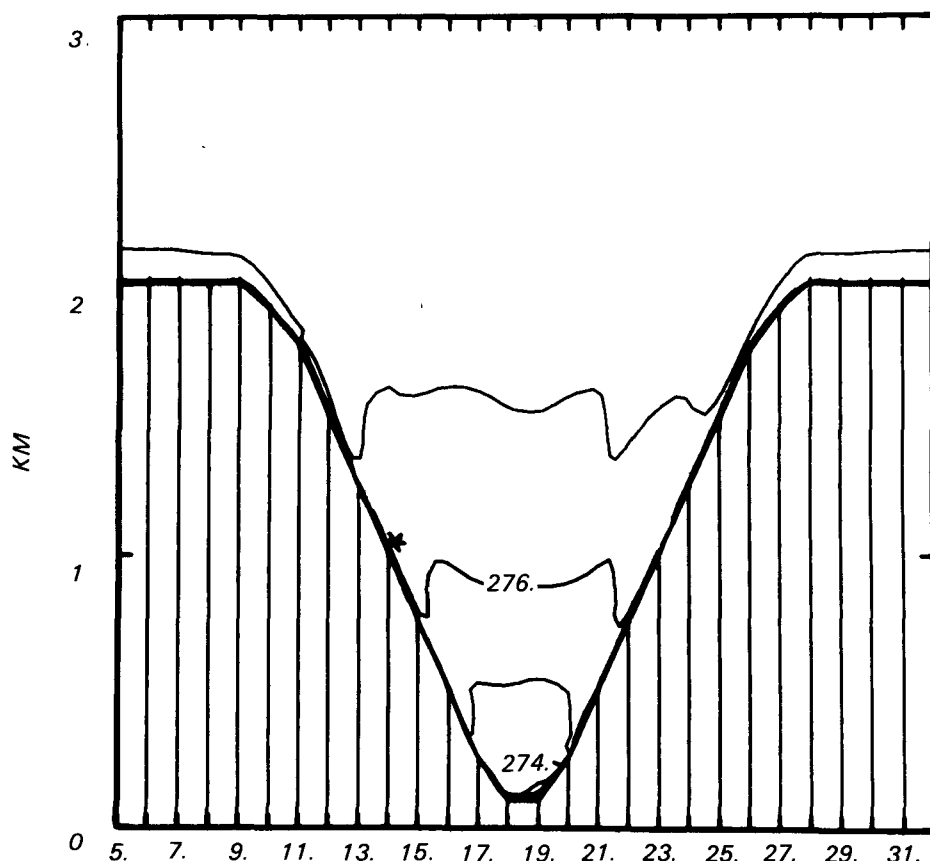


Figure 4a. Contours of potential temperature at 2330 LST ($\gamma = 23$). Contour interval is 1 K.

Boundary Layer. *Bound.-Layer Meteor.*, 15, 1241-1251.

Defant, F., 1951. Local Winds. In: *Compendium of Meteorology*. Amer. Meteor. Soc., Boston, Mass. pp. 655-675.

Hanna, S.R., 1979. Some Statistics of Lagrangian and Eulerian Wind Fluctuations. *J. Appl. Meteor.*, 18. pp. 518-531.

Mahrer, Y. and R.A. Pielke, 1978. Test of an Upstream Spline Interpolation Technique for the Advective Terms in a Numerical Mesoscale Model. *Mon. Wea. Rev.*, 106. pp. 818-830.

McNider, R.T. and R.A. Pielke, 1979. Application of the University of Virginia Mesoscale Model to Pollutant Transport. *Proceedings of Fourth Symposium on Turbulence, Diffusion and Air Pollution*. Amer. Meteor. Soc., Reno, Nev.

McNider, R.T., S.R. Hanna, and R.A. Pielke, 1980. Subgrid Scale Plume

Dispersion in Coarse Grid Mesoscale Models. *Second Conference on Applications of Air Pollution Meteorology*. New Orleans, La.

McNider, R.T., and R.A. Pielke, 1981. Diurnal Boundary Layer Development Over Sloping Terrain. Submitted to *J. Atmos. Sciences*.

Paegle, J., W.G. Zdunkowski, and R.M. Welch, 1976. Implicit Differencing of Predictive Equations for the Boundary Layer. *Mon. Wea. Rev.*, 104. pp. 1321-1324.

Smith, F.B., 1980. Personal Communication on June 15, 1980.

Tuescher, L.H. and L.E. Hauser, 1974. Development of Modeling Techniques for Photochemical Air Pollution. EPA-650/4-74-003. pp. 91.

Whiteman, C.D., 1980. Personal Communication to University of Virginia. Nov. 19, 1980.

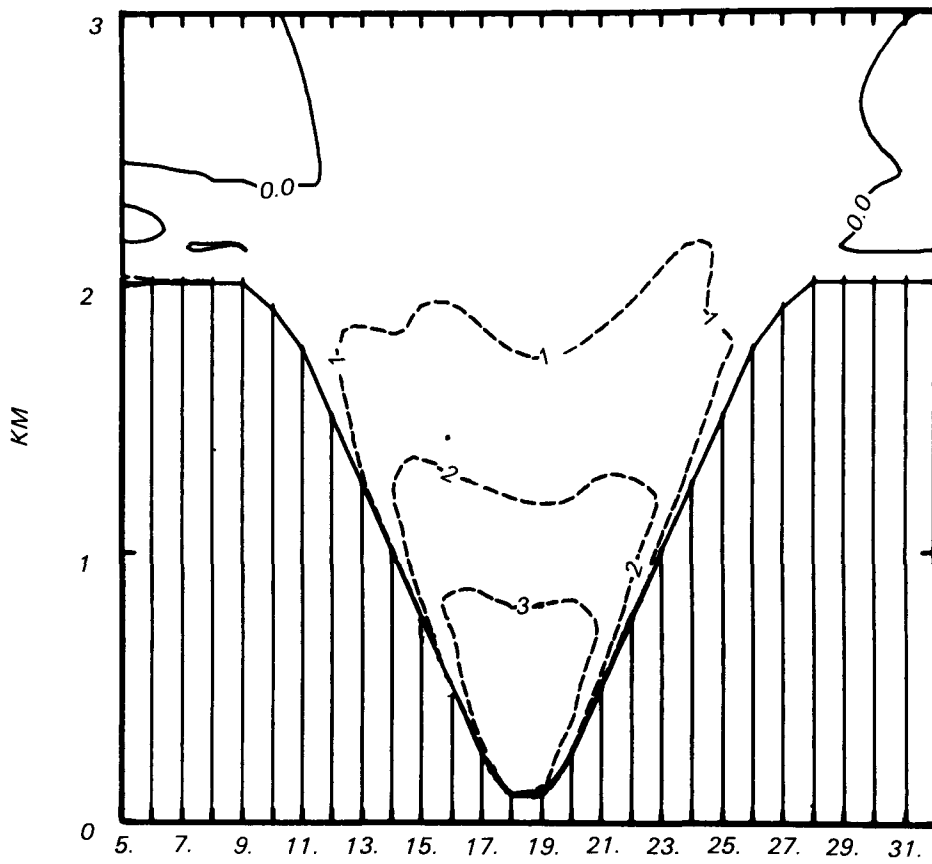
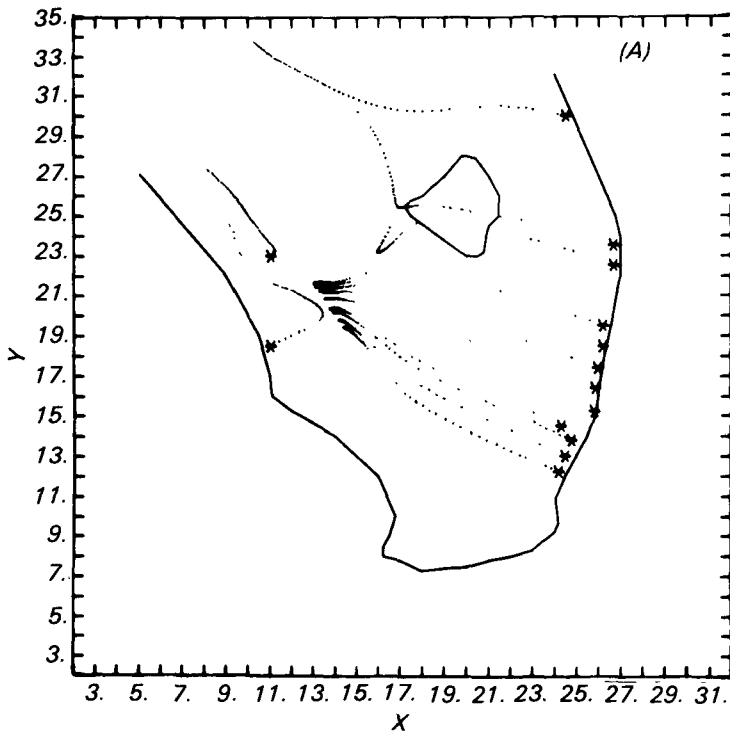
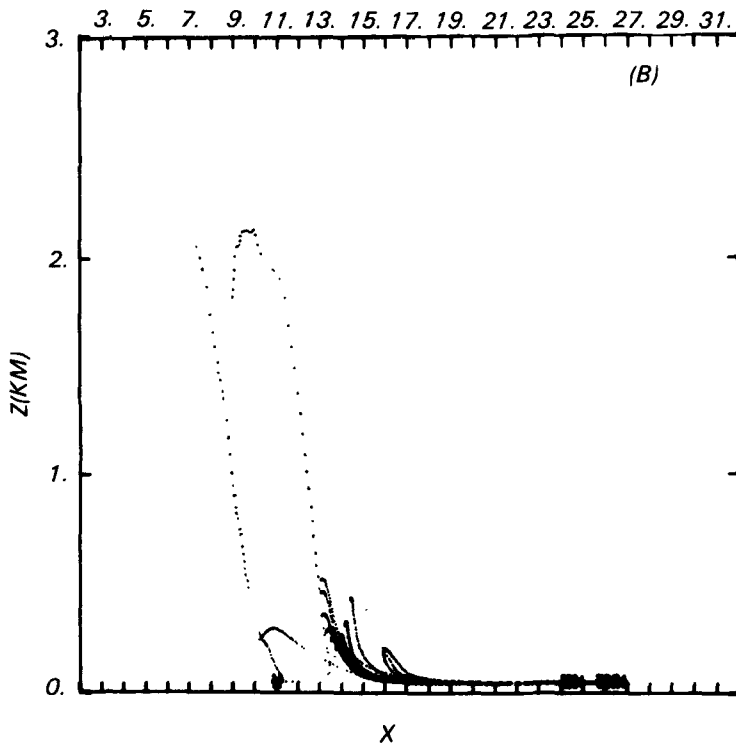


Figure 4b. Contours of the mountain wind (v-component) for the same time and location as 4a. Contour interval is 1 m/s.



(A) Plan view showing x-y distributions of particles.

Figure 5a. Particle streaklines at 1900 EST from 50-m release heights.



(B) Vertical view, looking northward, showing x-y distributions of particles. Particles were released at 10-min intervals, beginning at sunrise.

Figure 5b. Particle streaklines at 1900 EST from 50-m release heights.

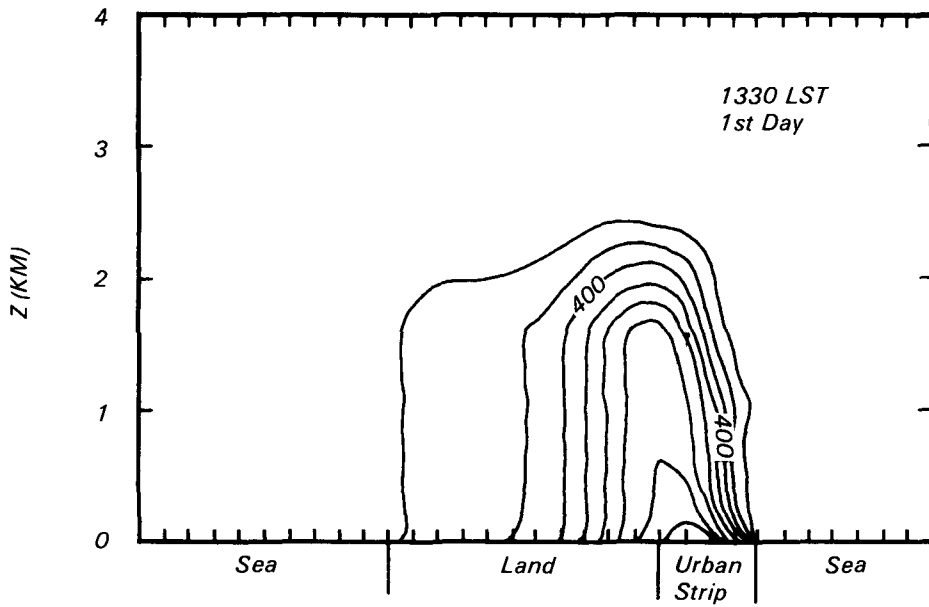


Figure 6a.

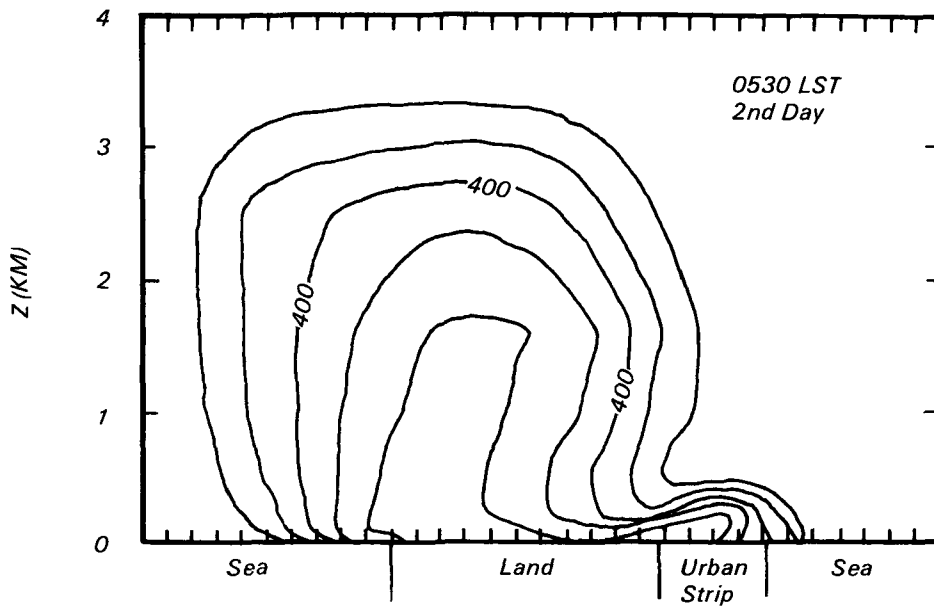


Figure 6b.

Figure 6. Contours of particle concentrations in a two-dimensional version of the mesoscale model. Synoptic flow is from the east (R). Particles are emitted over land areas and the urban strip. Figure 6a shows particles well-mixed within the convective boundary layer, while Figure 6b shows capture of particles within the nocturnal boundary layer carried out to sea in a shallow land breeze.

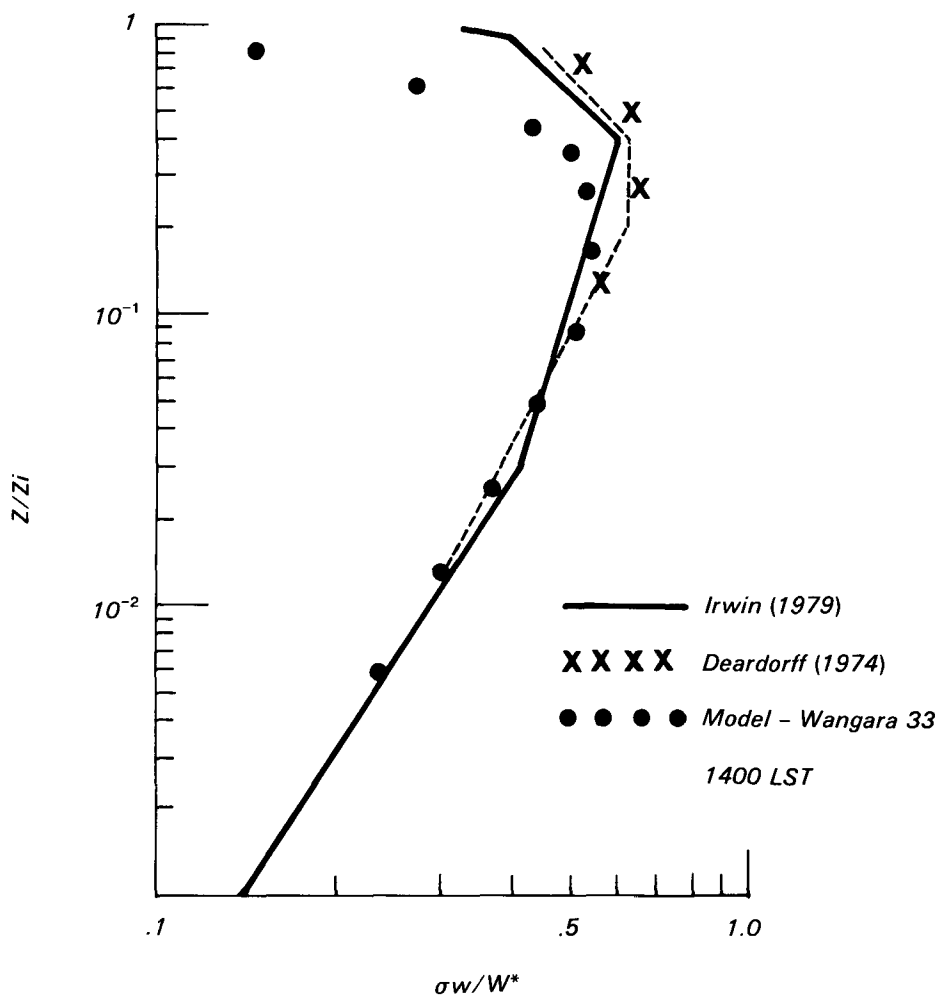


Figure 7. Plot of model-extracted, scaled σ_w in the planetary boundary layer, compared to observational composites and the numerical study by Deardorff (1974). The dashed line was extracted from an unpublished study by F. B. Smith of the British Meteorological Service. (w^* is the convective velocity scale given by $w^* = \mu^* (-h/kf)^{1/3}$).

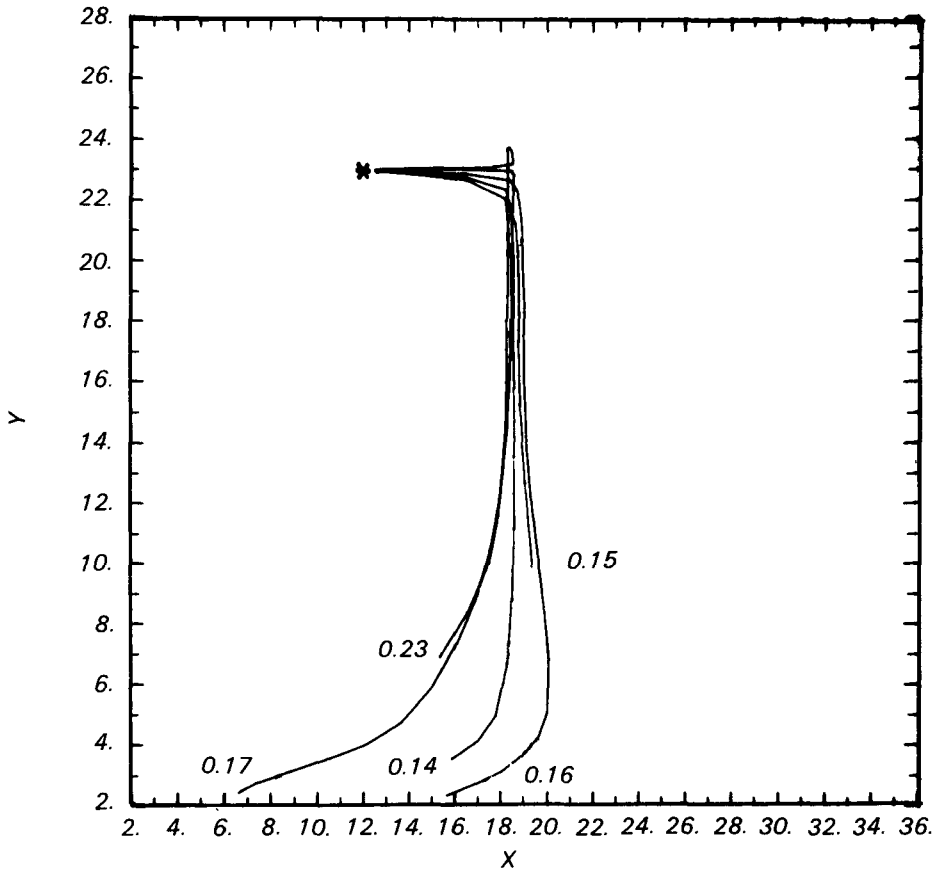


Figure 8. Trajectories of particles released an hour apart from a height of 2 m. Final heights (in km) are given on the side of the end of each trajectory.

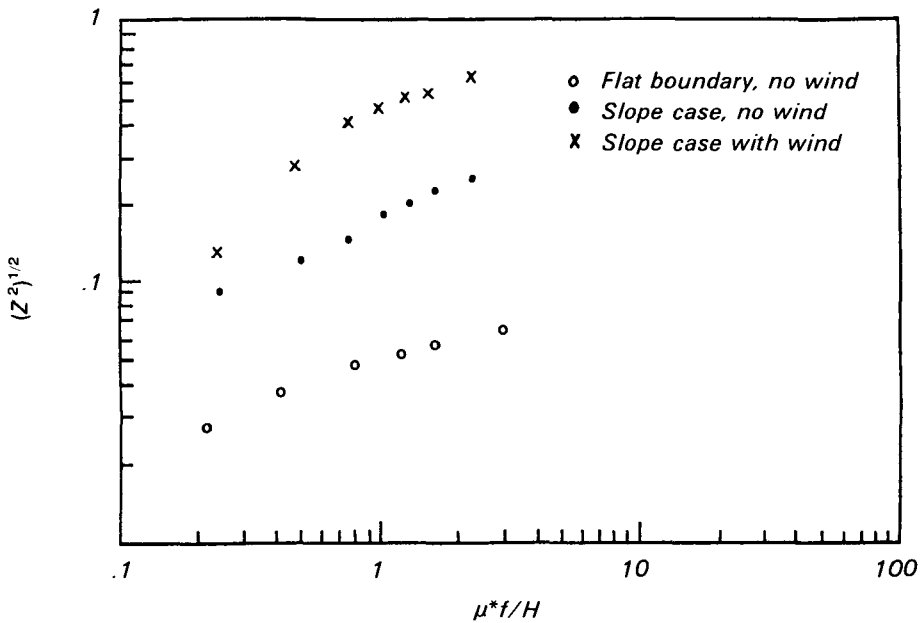


Figure 9. Vertical dispersion of the three cases described. Root-mean-square spread is scaled by the boundary layer height.

Richard T. McNider and Roger A. Pielke are with the Department of Environmental Sciences, University of Virginia, Charlottesville, VA 22903.

George C. Holzworth is the EPA Project Officer (see below).

The complete report, entitled "Impact of Topographic Circulations on the Transport and Dispersion of Air Pollutants," (Order No. PB 82-102 435; Cost: \$17.00, subject to change) will be available only from:

National Technical Information Service

5285 Port Royal Road

Springfield, VA 22161

Telephone: 703-487-4650

The EPA Project Officer can be contacted at:

Environmental Sciences Research Laboratory

U.S. Environmental Protection Agency

Research Triangle Park, NC 27711

ntar Protection

Information
Cincinnati OH 45268

Fees Paid
Environmental
Protection
Agency
EPA-335



Business
Private Use, \$300

PS 0000329
U S ENVIRONMENTAL PROTECTION AGENCY
REGION 5 LIBRARY
230 S DEARBORN STREET
CHICAGO IL 60604